CLAST ATTRIBUTES OF MARTIAN BOULDER HALOS: SEMI-AUTOMATED BOULDER SEGEMENTATION AND GEOCHEMICAL FINGERPRINTING OF REGIONAL HALO ATTRIBUTES.

J.S. Levy[1], S. Nerozzi[2], S. Mikus[1], F. Ishraque[1], M. Tebolt[3], J. Holt[2], [1]Colgate University, 13 Oak Ave., Hamilton, NY, jlevy@colgate.edu, [2]University of Arizona, Tucson, AZ. [3]University of Texas at Austin.

Introduction: Boulder halos are largely concentric rings or annuli of boulder-sized (>0.5 m diameter) clasts present across the middle latitudes on Mars [1]. Because they are associated with circular fracture and trough patterns or wide, low-relief depressions similar to impact craters, they have been inferred to form as a result of excavation of boulders from beneath an overlying fine-grained and/or ice-rich mantle [2-6]. Even if boulders are excavated from beneath a recent-Amazonian-aged, ice-rich mantling layer, the origin of those boulders remains unknown. Are boulders pre-existing rock fragments that are present as regolith beneath fine-grained niveoaeolian mantles [7]? Or are they fractured underlying bedrock that has been excavated and brought to the surface during the impact event? Two approaches can be brought to bear to address these competing hypotheses: 1) measuring boulder halo clast size-frequency distributions in order to assess whether halo boulders share a fragmentation size distribution associated with fresh impact crater ejecta, and 2) comparing the geochemical attributes of boulder halo sites and halo-free surfaces in order to determine if they share Gamma Ray Spectrometer (GRS)-discernable compositions, reflecting regional patterns of bedrock and/or regolith composition.

Methods: Both investigations reported here made use of the boulder halo catalog in [1]. HiRISE images between ~50-80° were classified as either containing or not containing boulder halos based on inspection.

GRS Mapping. We use near subsurface (<1 m depth) elemental concentration data derived from the Mars Odyssey GRS, available in 2°x2° and 5°x5° longitude-latitude grids on the Planetary Data Science node. The original gridded data are noisy, so we applied a running circular averaging function to decrease uncertainty. In this process, we added weights as a function of the distance from the center of the averaging circle based on a Gaussian curve and the 50% signal radii for each element [8]. The validity of a Gaussian function to calculate averaging weights is supported by the spatial covariance analysis of raw gridded GRS data in ESRI ArcGIS, and the broad spatial sampling of the GRS detector [9]. The radius of the running average extends to the 95% signal radius. Then, we extracted concentration values of each available element (i.e. Cl, Fe, H, K, Si and Th) at all boulderiferous and non-boulderiferous study sites in [1]. The averaging process expands the latitudinal bounds of elemental concentration data that don't have global coverage (Cl, Fe, H and Si) at the expense of increased uncertainty.

Automated Boulder Segmentation. Boulder identification was conducted using a customized ArcGIS object-based classification workflow (Fig. 1). Raster analysis requires a careful pre-assessment of the HiRISE image in order to determine the range of pixel DN values encompassed by the boulders—which can stand out as bright features on a dark surface, or dark features on a bright background. Three segmentation parameters are adjusted for each candidate halo: spatial detail (the degree to which the desired features are clustered), minimum segment size (depends on the resolution of the raster: for 25 cm data, we use 4 pixels to map only 1+ m boulders), and spectral detail (a measure of internal variability within segments).

Results: *GRS Mapping.* Northern sites with no boulder halos are enriched in K and Th compared to boulderiferous sites in the same hemisphere, and all southern locations (Fig. 2). We do not detect significant variability in the concentrations of Cl, Fe, H and Si.

Automated Boulder Segmentation. Changing the spectral detail has limited/no effect on presence of false positive results (circled black in Fig. 1), but has a significant effect on presence of false negative results (circled red). Instead, the pixel intensity threshold has a strong effect on automated boulder detection: higher bounding DNs means the process becomes more selective towards bright boulders, leaving out smaller, dimmer rocks. Although this increases the number of false negatives, it also reduces the amount of false positives.

Discussion: *GRS Mapping.* We hypothesize that impacts forming boulder halos in the northern hemisphere exhume bedrock fragments that are depleted in K and Th compared to materials found near the surface. Similar concentrations of K and Th between all southern sites and northern boulderiferous sites suggests that the deeper bedrock in the northern hemisphere is of similar composition to the terrains of the southern highlands, and is distinct from shallow capping lavas. The enrichment of K and Th in northern plains surficial materials at non-halos sites could be the result of weathering of older rocks and/or a source rock that is richer in these elements, and thus is possibly more evolved compared to the underlying layers. The lack of variability in the concentration of Cl and other elements suggests that the boulder halo formative processes do not alter the composition of impacted rocks and sediments significantly.

Ongoing Work: Next steps for this project focus on linking automated boulder segmentation size/fre-

quency distributions to young crater production functions (e.g., [10]) for fresh impact craters to assess the role of boulder breakdown and reworking.

Acknowledgements: This work was supported in part by NASA award NNX16AJ41G.

References: [1] Levy, J. S. *et al.*(2018) *JGR Planets* **123,** 322–334. [2] Barata, T., et al. (2012) *PSS***,** 62–69. [3] Kostama, V. P., et al. (2006) GRL, **3,** L11201. [4] Levy, J. S., et al. (2008) LPSC doi:10.1029/-2001JE001831. [5] Orloff, T., et al., (2011) *JGR Planets* **116,** E11006. [6] Korteniemi, J. & Kreslavsky, M. A. (2013) *Icarus* **225,** 960–970. [7] Head, J. W., et al. (2003) *Nature* **426,** 797–802. [8] Boynton, W.V. et al. (2007) *JGR Planets*, 112. [9] Boynton, W.V. et al. (2004) *2001 Mars Odyssey*, 322-334. [10] Watkins, R.N. et al. (2019) *JGR Planets*, 10.1029/2019JE005963

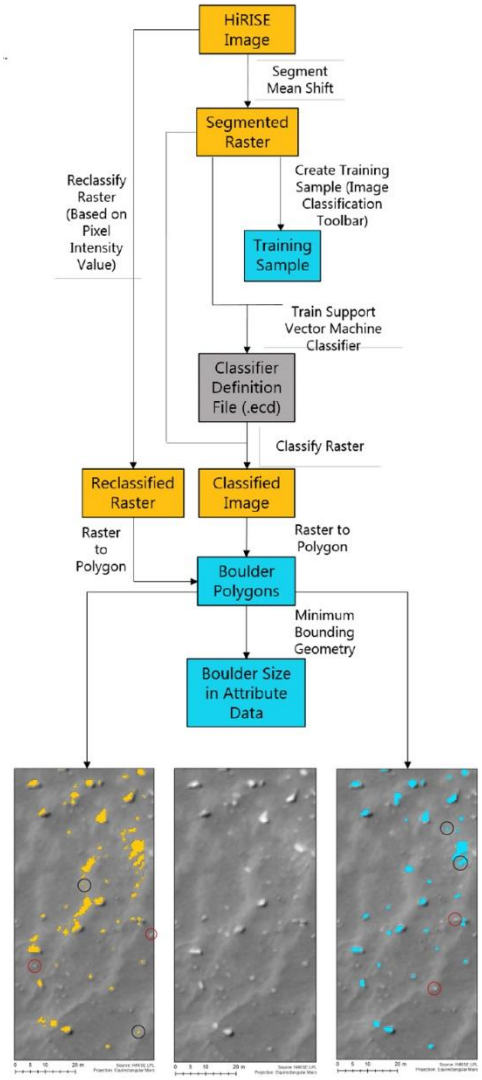

Fig. 1. (Right) Workflow for object-based boulder detection using ArcGIS. Semi-automated detection produces boulder size and location data based on minimum bounding geometry of bright boulder surfaces. False positive results are circled black, false negatives in red. Thresholding and spectral detail settings largely control false-negative characterization.

Fig.2 (Below) Figure 1: Extracted GRS elemental concentrations for sites with and without boulder halos in the north and south hemisphere of Mars. Southern hemisphere halos are few in number, producing few differences between halo and non-halo sites. K and Th are both enriched at non-halo sites in the northern hemisphere, suggesting that either depleted material is being excavated by boulder halos, or that boulder halos preferentially form when K and Th depleted bedrock are available to be excavated.